J. Fluid Mech. (1990), *vol.* 220, *pp.* 515–537
Printed in Great Britain

Turbulent dispersion of particles in self-generated homogeneous turbulence

By R. N. PARTHASARATHY† AND G. M. FAETH‡
Department of Aerospace Engineering, The University of Michigan, Ann Arbor, MI 48109-2140, USA

(Received 6 October 1989)

Turbulent dispersion of particles in their self-generated homogeneous turbulent field was studied both experimentally and theoretically. Measurements involved nearly monodisperse spherical glass particles (nominal diameters of 0.5, 1.0 and 2.0 mm) falling with uniform particle number fluxes in a nearly stagnant water bath. Particle Reynolds numbers based on terminal velocities were 38, 156, and 545 for the three particle sizes. The flows were dilute with particle volume fractions less than 0.01%. Measurements included particle motion calibrations, using motion-picture shadowgraphs; and streamwise and cross-stream mean and fluctuating particle velocities, using a phase-discriminating laser velocimeter. Liquid-phase properties were known from earlier work. Particle properties were predicted based on random-walk calculations using statistical time-series methods to simulate liquid velocities along the particle path.

Calibrations showed that particle drag properties were within 14% of estimates based on the standard drag correlation for spheres, however, the particles (particularly the 1.0 and 2.0 mm diameter particles) exhibited self-induced lateral motion even in motionless liquid due to eddy-shedding and irregularities of shape. Particle velocity fluctuations were primarily a function of the rate of dissipation of kinetic energy in the liquid since this variable controls liquid velocity fluctuations. Streamwise particle velocity fluctuations were much larger than cross-stream particle velocity fluctuations (2–5:1) largely due to varying terminal velocities caused by particle size variations. Cross-stream particle and liquid velocity fluctuations were comparable owing to the combined effects of turbulent dispersion and self-induced motion. Predicted mean and fluctuating particle velocities were in reasonably good agreement with the measurements after accounting for effects of particle size variations and self-induced motion. However, the theory must be extended to treat self-induced motion and to account for observations that this motion was affected by the turbulent environment.

1. Introduction

The objective of this investigation was to study the turbulent dispersion of particles moving in their self-generated homogeneous turbulent field. This process is important in dispersed multiphase flows when direct modification of continuous phase turbulence properties by transport from the dispersed phase, called turbulence modulation by Al Taweel & Landau (1977), is significant. Such conditions are encountered in the dense regions of sprays as well as in dilute dispersed flows when mean velocity gradients are small, e.g. the flow field within liquid- or particle-

† Present address: Institute of Hydraulic Research, University of Iowa, Iowa City, IO, USA.
‡ Author to whom correspondence should be addressed.

containing rocket engines as well as in natural phenomena like rainstorms. The study involved a homogeneous dilute particle-laden flow generated by a uniform flux of particles settling under the force of gravity in a nearly stagnant (in the mean) liquid bath. A companion study considered the continuous-phase properties of these flows (Parthasarthy & Faeth 1990); the emphasis of the present study was to investigate the dispersed-phase properties both theoretically and experimentally.

Early studies of the turbulent dispersion of particles concentrated on the small-particle limit where the relative velocities between the phases are small and particle mixing can be approximated by single-phase scalar mixing through the locally-homogeneous-flow approximation, see Faeth (1987) for a review of past work along these lines. The locally-homogeneous-flow approximation is of limited value, however, since most practical dispersed multiphase flows involve significant relative velocities between the phases and dispersed-phase elements do not remain associated with particular fluid elements. This phenomenon was recognized by Yudine (1959) and Csanady (1963) and is called the 'crossing trajectories' effect, i.e. dispersed-phase elements and fluid elements follow different trajectories and only interact for a time. Katz (1966) and Meek & Jones (1973) report early applications of these ideas to the study of the dispersion of heavy particles in the atmosphere. Other work, at the Stokes limit for particle motion and with various approximations for the continuous phase of simple turbulent flows, includes Reeks (1977, 1980), Pismen & Nir (1978), Nir & Pismen (1979), Gouesbet, Berlemont & Picart (1984), Desjonqueres *et al.* (1986) and Maxey (1987). All these studies find significant effects of finite relative velocities between the phases.

Most practical dispersed flows, as well as past experiments, involve dispersed-phase Reynolds numbers beyond the Stokes limit. Numerous measurements of continuous- and dispersed-phase properties have been reported for sprays and other turbulent shear flows, see Faeth (1987) for a summary of recent work; however, homogeneous flows involve fewer complications for the interpretation of turbulent dispersion phenomena and will be emphasized here. Snyder & Lumley (1971) completed measurements of turbulent dispersion of single particles in the isotropic decaying turbulent flow downstream of a grid: this study has served as a primary source of data for developing models of the process. Wells & Stock (1983) studied turbulent particle dispersion in a similar arrangement, using charged particles in an electric field so that effects of relative velocities (crossing trajectories) could be separated from particle inertia: they found that inertia influenced particle velocity fluctuations but concluded that particle dispersion was primarily influenced by crossing trajectories for their test conditions. Ferguson & Stock (1986) also studied particle dispersion in grid-generated turbulence, further highlighting effects of crossing trajectories. Taken together, these results demonstrate the importance of both particle and continuous-phase properties on turbulent dispersion; therefore, the process does not lend itself to empirical correlation and must be understood at a fundamental level before reliable estimates of turbulent dispersion can be achieved.

Numerous models of turbulent dispersion in dilute dispersed flows have appeared but recent work has emphasized stochastic simulations as a way of providing for the nonlinear interactions between the phases in a relatively fundamental way. This involves random-walk calculations of dispersed-phase trajectories coupled with a simulation of the properties of the continuous phase. Methods involving turbulence modelling concepts have been widely reported and have exhibited capabilities to match existing measurements for simple shear flows (Crowe 1982; Faeth 1987). However, the *ad hoc* features of these models are not very satisfying and recent work

has sought more fundamental methods. Maxey (1987) and Picart, Berlemont & Gouesbet (1986) describe representative work along these lines for dilute isotropic turbulent flows. Maxey (1987) computes the motion of particles at the Stokes limit in a constant density flow generated as a finite series of randomly selected Fourier modes following Kraichnan (1970). This is a reasonable approximation that is much simpler than direct numerical simulation of turbulence. However, extending this approach to practical shear flows will require substantial advances of computer capabilities. The approach of Picart *et al.* (1986) is somewhat more general and involves approximate simulation of turbulence properties only along the particle trajectory – yielding good predictions of the Snyder & Lumley (1971) measurements. This approach is closely related to well-developed methods of statistical time-series simulations described by Box & Jenkins (1976), although Picart *et al.* (1986) do not note this analogy.

The objective of the present investigation is to consider turbulent particle dispersion in homogeneous turbulent fields generated solely by particle motion through a nearly stagnant (in the mean) liquid bath. Unlike grid-generated isotropic turbulence, this flow is formally stationary and exhibits levels of anisotropy that are typical of dispersed multiphase flows (Faeth 1987). Measurements of liquid-phase properties of these flows have been reported by Parthasarathy & Faeth (1990); the present study completes the description of these flows by providing measurements of dispersed-phase properties. Finally, flow properties are predicted along the lines of Picart *et al.* (1986) except that methodology from statistical time-series simulations is adopted in order to take advantage of past work in this field (Box & Jenkins 1976).

Experimental and theoretical methods are described in the next two sections. Measured and predicted results are then presented in §4, considering mean and fluctuating particle velocities, particle velocity probability density functions (p.d.f.s) and the sensitivity of predictions to variations of parameters in the formulation, in turn. Major conclusions of the study are summarized in §5. Additional details and a complete tabulation of data can be found in Parthasarathy (1989).

2. Experimental methods

2.1. *Apparatus*

The experimental apparatus and its evaluation are described by Parthasarathy & Faeth (1990) and will be considered only briefly here. The flow was generated by a variable-speed particle feeder which delivered particles to an array of screens to provide a uniform particle flux. The particles then fell into a windowed tank ($410 \times 535 \times 910$ mm) filled with water to a depth of 800 mm. The particles reached terminal velocities within 100–200 mm of the liquid surface while measurements were made at the centre of the tank. The particles collected naturally at the bottom of the tank, inducing a negligible displacement velocity of the liquid (less than 0.014 mm/s), and were removed from time to time using a suction system.

Tests to evaluate the uniformity of the flow, effects of tank volume and the time required to achieve stationary conditions are described by Parthasarathy & Faeth (1990). The central region of the tank (300×300 mm cross-section for a range of heights extending ± 100 mm from the measuring location) had particle number fluxes and liquid velocity fluctuations that were uniform while Reynolds stresses were essentially zero, within experimental uncertainties (10% for fluxes and velocity fluctuations, 50% for Reynolds stresses). Effects of stabilizing waves at the liquid surface with a honeycomb were negligible while reducing the bath volume by a factor

of 32, using Plexiglas partitions and reducing liquid depths, also caused less than a 10% variation of liquid velocity fluctuations. Thus, the arrangement provided a homogeneous flow with relatively little effect of the bath surfaces on flow properties.

2.2. *Instrumentation*

Streamwise and cross-stream mean and fluctuating particle velocities were measured using the phase-discriminating laser velocimeter (LV) described by Parthasarathy & Faeth (1990). This involved a fixed LV channel, based on the 514.5 nm line of a 2 W argon-ion laser, operating in the dual-beam forward-scatter mode. Directional bias and ambiguity were eliminated using a 40 MHz Bragg-cell frequency shifter with the output signal downshifted to convenient frequency ranges for filtering and signal processing. Streamwise and cross-stream velocities were measured by rotating the LV optics accordingly. A beam spacer provided an initial 9 mm beam spacing while the receiving optics were shifted to 45° from the forward-scatter direction to minimize problems of large pedestal signals from the particles. This yielded a fringe spacing of 14.3 μm and an optical measuring volume that was 300 μm in diameter and 300 μm long (the actual measuring volume was increased from this size by the particle dimensions since grazing collisions were recorded). The LV signals were interpreted using a burst-counter signal processor (TSI Model 1980B).

The phase discrimination system involved a third beam from a 5 mW HeNe laser (at an angle of 18° from the LV axis), which enveloped the LV measuring volume, and collection optics set off-axis (at an angle of 32° from the LV axis). The region viewed by the discriminator (0.6 mm diameter and 1.3 mm long) surrounded the LV measuring volume. Particle velocity measurements were made with the water unseeded and the detector operated at low gain which only responded to large-amplitude signals from particles. Thus, the discriminator system was only used to validate the presence of a particle when the signal was recorded. Operation was confirmed by ending the flow of particles which invariably caused the data rate of the LV processor to return to zero. Particle arrival rates were low (10–80 per hour). Number averages of mean and fluctuating velocities were obtained over 200–500 particles.

Parthasarathy (1989) evaluated the experimental uncertainties (95% confidence) of these measurements, as follows: mean streamwise particle velocities; less than 6%; mean cross-stream particle velocities, less than 41%; fluctuating streamwise particle velocities, less than 11%; and fluctuating cross-stream particle velocities, less than 16%. These uncertainties were largely dominated by finite sampling times.

2.3. *Particle properties*

2.3.1. *Particle size*

Glass particles having nominal diameters of 0.5, 1.0 and 2.0 mm, and a density of 2450 kg/m^3, were used for the tests. The size distributions of the 0.5 and 1.0 mm diameter particles were measured under a microscope with experimental uncertainties (95% confidence) of less than 10% near maximum probability conditions; the size distribution of the 2.0 mm diameter particles was measured using a vernier calliper with experimental uncertainties (95% confidence) of less than 5% near the maximum probability condition. The resulting p.d.f.s of particle diameter are plotted as a function of normalized diameters in figure. 1. The measurements for the three particle sizes follow Gaussian distributions within experimental uncertainties. Standard deviations are roughly 10% of the nominal diameter of the particles: actual values of the standard deviations will be taken up later.

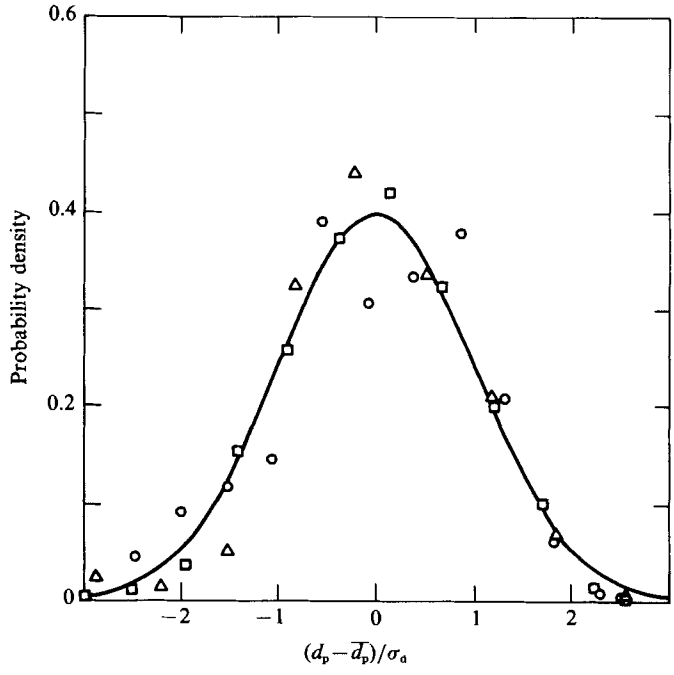

FIGURE 1. Probability density functions of particle diameters. □, $d_p = 0.5$ mm; ○, $d_p = 1.0$ mm; △, $d_p = 2.0$ mm; ——, Gaussian distribution.

These measurements also showed that the particles were not all spherical. The degree of ellipticity (ratio of the major to the minor diameter) increased with increasing nominal particle diameter, as follows: 20% of the 0.5 mm diameter particles were ellipsoids with a mean ellipticity of 1.05; 40% of the 1.0 mm diameter particles were ellipsoids with a mean ellipticity of 1.15; and 65.5 of the 2.0 mm diameter particles were ellipsoids with a mean ellipticity of 1.25.

2.3.2. *Particle drag*

The drag coefficients of the particles were calibrated by measuring the terminal velocities of individual particles settling in a motionless bath with the LV. A single-particle feeder described by Parthasarathy (1989) was used for these tests: it delivered particles to a glass tube (4 mm inner diameter) that ended 150 mm above the LV measuring volume. The time intervals between particles were in the range 20–50s. It was necessary to aim the particles with the glass tube to get adequate velocity samples in a reasonable length of time; however, calculations showed that the particles reached their terminal velocities within 60 mm of the point of release so that the particle feeder did not affect terminal velocities. Liquid velocity measurements also showed that disturbances of the bath due to previous particles were small for the separation times between particles used for these measurements.

The LV system was similar to the arrangement described for particle velocity measurements in the homogeneous turbulent flow, however, a large-diameter aperture (2 mm) was used on the detector to increase signal rates. The results were summarized as p.d.f.s of particle velocities for the three particle sizes. The uncertainties of these measurements were less than 9% near the maximum probability condition, largely governed by the number of samples.

Predictions of the p.d.f.s of terminal velocities were also undertaken as the first step in developing the analysis of particle velocities in the homogeneous turbulent flow. These predictions were based on the measured p.d.f.s of particle diameter, illustrated in figure 1, assuming spherical particles at the terminal velocity condition in a quiescent liquid. Under these conditions the terminal velocity, U_∞, of a particle having a diameter d_p is as follows:

$$U_\infty = (4gd_p(\rho_p/\rho - 1)/(3C_D))^{\frac{1}{2}}, \tag{1}$$

where g is the acceleration due to gravity, ρ_p and ρ are the particle and liquid densities, and C_D is the drag coefficient. C_D was found from the standard drag curve for spheres (Putnam 1961)

$$C_D = 24(1 + \tfrac{1}{6}Re^{\frac{2}{3}})/Re, \tag{2}$$

where the particle Reynolds number is defined as follows:

$$Re = U_\infty d_p/\nu, \tag{3}$$

and ν is the kinematic viscosity of the liquid. Equation (2) is limited to $Re < 1000$ which is satisfactory for present test conditions.

The calibration was completed by matching the predicted and measured most probable terminal velocity by multiplying the standard drag correlation of (2) by a fixed constant for each nominal particle size, as follows: 1.14 for the 0.5 and 2.0 mm diameter particles, and 1.00 for the 1 mm diameter particles. These corrections are surprisingly small in view of the ellipticities of some of the particles and anticipated uncertainties of the standard drag correlation (Clift, Grace & Weber 1978).

The predicted and measured p.d.f.s of the normalized terminal velocities for the three particle sizes are illustrated in figure 2 (normalization parameters will be taken up later). After the minor corrections of the drag coefficients that were just noted, the comparison between predictions and measurements is quite good. This implies that particle diameter variations are responsible for most of the variance of the terminal velocities of the particles. Since the corrections of the standard drag correlation were small, and the p.d.f.s of terminal velocities were reasonably good based on the corrected drag expression, this expression was used for all subsequent calculations of particle drag.

2.3.3. *Self-induced motion*

It was found that particles dropped individually into a still bath did not fall straight; instead, there was cross-stream motion which increased with increasing particle diameter. This behaviour was calibrated since self-induced motion influences particle velocity fluctuations and affects the interpretation of turbulent dispersion results.

Measurements of self-induced motion with the LV were not possible since sampling rates were too low; therefore, these velocities were measured from shadowgraph motion pictures of individual particles falling in a still bath. The single-particle feeder, without the glass tube, was used to release individual particles into the bath. A shadowgraph motion picture of the falling individual particles, having a field view of 250 mm, was obtained with a Redlakes LOCAM camera using Kodak Tri-X Reversal film (ASA 400). The film was projected frame-by-frame on a screen having a grid so that particle tracks could be followed and recorded. The particle displacement tracks were differentiated numerically to find particle velocities using a central-difference scheme. Mean and fluctuating streamwise and cross-stream particle velocities were calculated by averaging over 50 particle paths. Uncertainties

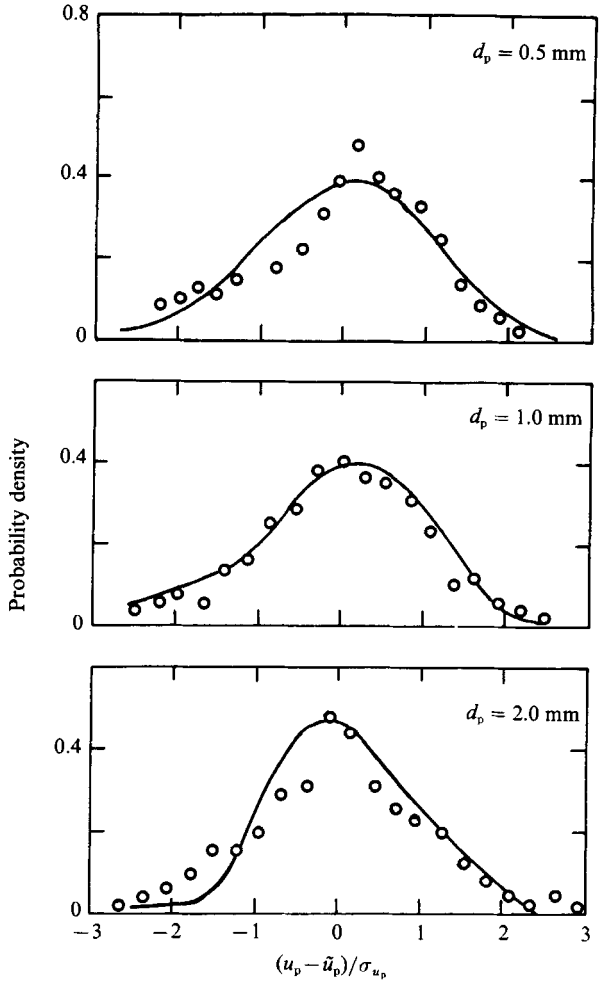

FIGURE 2. Probability density functions of terminal velocities: ○, data; ——, predictions.

(95% confidence) of these measurements were largely governed by sampling limitations and were less than 15% for mean streamwise velocities and less than 30% for velocity fluctuations.

The mean and fluctuating particle velocities due to self-induced motion are summarized in table 1 for the three particle sizes. The mean terminal velocities from these particle track measurements agreed with the LV measurements made during the particle drag calibrations within the experimental uncertainties of each (10%).

The particle velocity fluctuations due to self-induced motion, summarized in table 1, represent variations along particular particle paths so that effects of terminal velocity changes due to diameter variations within a particular size group are small. The streamwise velocity fluctuations due to self-induced motion for the 0.5, 1.0 and 2.0 mm diameter particles are 2.8, 0.96 and 0.19% of the mean terminal velocities; in comparison, the apparent streamwise velocity fluctuations due to size variations are 10.8, 9.5 and 6.1% for the same three particle sizes. Thus, particle velocity fluctuations in the streamwise direction were dominated by effects of particle size variations and turbulent dispersion while effects of self-induced particle motion were small for this component of velocity. The self-induced cross-stream particle velocity

Particle diameter (mm)	0.5[a]	1.0[a]	2.0[a]	2.0[b]
$\tilde{u}_p$ (mm/s)	71	157	270	274
$(\tilde{u}''^2_{ps})^{\frac{1}{2}}$ (mm/s)	2.0	1.5	0.5	0.5
$(\tilde{v}''^2_{ps})^{\frac{1}{2}}$ (mm/s)	1.1	5.6	13.5	13.1

[a] Measurements based on individual particles dropped near the water surface.
[b] Measurements based on individual particles dropped through the dispersing screen arrangement.

TABLE 1. Summary of self-induced particle motion properties

fluctuations, however, are significant – particularly for the 1.0 and 2.0 mm diameter particles where particle Reynolds numbers exceed 150. Two factors probably contributed to this behaviour: unsteady lateral forces on the particles due to eddy shedding at higher terminal particle Reynolds number (Nakamura 1976; Viets 1971), and effects of increased ellipticity with increasing particle size.

In view of the combined effects of streamwise particle velocity fluctuations caused by size variations and cross-stream particle velocity fluctuations caused by self-induced motion, observations of cross-stream particle velocity fluctuations for the 0.5 mm diameter particles provide the best indication of effects of turbulent dispersion for the present test conditions. Results for the larger particle sizes will still be considered, however, since it is of interest to study whether the turbulent field of the particle-laden flow influences self-induced motion, which is large for these particle sizes.

Measurements were also undertaken to determine whether the dispersing screens induced any cross-stream motion of the particles. This was a concern since the impact of the particles on the screens could cause the particles to spin, generating Magnus forces which would deflect the particles in the cross-stream direction. This effect was studied by dropping particles individually through the dispersing screen arrangement and measuring particle velocities using shadowgraph motion pictures. Results of these experiments for the 2.0 mm diameter particles are also summarized in table 1. The measurements of mean and fluctuating velocities of the particles passing through the screen arrangement are seen to be almost the same as for single particles dropped directly into the bath; therefore, the dispersing screen did not modify particle properties appreciably.

2.4. *Test conditions*

A range of particle number fluxes were considered for each particle size: representative test conditions at the low and high ends of these ranges are summarized in table 2. Particle properties are emphasized in table 2; additional information about liquid-phase properties can be found in Parthasarathy & Faeth (1990) for the same test conditions. The properties of the particle size and terminal velocity distributions that were discussed earlier are summarized at the top of the table. Mean streamwise particle velocities within the particle-generated turbulent field of the bath, $\tilde{u}_p$, were the same as terminal velocities in a still liquid, within experimental uncertainties.

Mean particle spacings, l_p, were found by assuming that particles were falling randomly with a uniform particle number flux, $\dot{n}''$, at the mean particle terminal velocity, yielding

$$l_p = (\tilde{u}_p/\dot{n}'')^{\frac{1}{3}}. \tag{4}$$

Particle diameter (mm)	0.5 (0.045)		1.0 (0.085)		2.0 (0.15)	
Particle loading	Low	High	Low	High	Low	High
Particle properties:						
Terminal velocity (mm/s)[a]	65 (7)		147 (14)		262 (16)	
Reynolds number(−)	38		156		545	
Number flux (kpart/m^2 s)	55.4	110.8	3.7	20.9	1.1	3.3
Mean spacing (mm)	10.5	8.2	32.7	18.3	61.8	43.2
$\tilde{u}_p$ (mm/s)	66.8	71.5	144.2	139.0	265.0	265.0
$(\tilde{u}_p''^2)^{\frac{1}{2}}$ (mm/s)	11.0	12.1	17.0	21.9	19.0	20.5
$(\tilde{v}_p''^2)^{\frac{1}{2}}$ (mm/s)	2.7	4.4	2.5	7.4	7.8	9.8
Liquid properties:						
Rate of dissipation (mm^2/s^2)	53.2	106.3	27.3	155.8	61.7	193.5
$\bar{u}$ (mm/s)	1.6	3.9	1.0	3.8	3.0	6.0
$\bar{v}$ (mm/s)	0.7	0.6	1.1	1.6	1.0	0.9
$(\bar{u}'^2)^{\frac{1}{2}}$ (mm/s)	3.3	4.7	2.4	5.1	3.7	6.1
$(\bar{v}'^2)^{\frac{1}{2}}$ (mm/s)	1.6	2.7	1.2	2.3	1.7	3.1

[a] Measured based on single particles dropped in a still bath during particle drag calibrations.

TABLE 2. Representative test conditions. Round glass beads, density of 2450 kg/m^3, falling in a stagnant water bath at 298 ± 2 k. Numbers in parentheses denote standard deviations. Particle volume fractions less than 0.01%, displacement velocities less than 0.014 mm/s, direct dissipation by particles less than 4.5%.

The resulting particle spacings were in the range 8–62 mm, or 16–33 particle diameters, yielding particle volume fractions less than 0.01%, therefore, effects of direct particle-to-particle interactions and collisions were negligible. Apparent streamwise particle velocity fluctuations, $(\tilde{u}_p''^2)^{\frac{1}{2}}$, were much larger than cross-stream particle velocity fluctuations, $(\tilde{v}_p''^2)^{\frac{1}{2}}$, owing to variations of terminal velocities caused by size variations, as noted earlier.

Following Parthasarathy & Feath (1990), the rate of dissipation of turbulence kinetic energy within the bath, ϵ, was used to characterize bath operating conditions for various particle sizes and number fluxes. ϵ was found by noting that mean particle velocities were constant and were much greater than particle velocity fluctuations (the ratio of $(\tilde{v}_p''^2)^{\frac{1}{2}}/\tilde{u}_p$ is most representative since effects of particle size variations are small for cross-stream velocity fluctuations). Then the rate of production of turbulence kinetic energy in the bath is equal to the rate of loss of potential energy of the particles as they fall through the bath, which in turn is equal to the rate of dissipation, i.e.

$$\epsilon = \pi \dot{n}'' g d_p^3 (\rho_p - \rho)/(6\rho). \tag{5}$$

Parthasarathy (1989) shows that direct dissipation by particles is small, less than 5%, so that dissipation primarily occurs within the particle wakes.

The particle flows generated mean streamwise and cross-stream velocities, $\bar{u}$ and $\bar{v}$, in the bath, as discussed by Parthasarathy & Faeth (1990); however, these velocities are small in comparison to the terminal velocities of the particles and they had little effect on particle motion. Streamwise and cross-stream liquid velocity fluctuations, $(\bar{u}'^2)^{\frac{1}{2}}$ and $(\bar{v}'^2)^{\frac{1}{2}}$, were largely functions of ϵ for present test conditions, with particle sizes and number fluxes being secondary factors (Parthasarathy & Faeth 1990). Particle and liquid velocity functions in the cross-stream direction are comparable so that effects of turbulent dispersion were significant for present test conditions.

3. Theoretical methods

3.1. *Particle motion*

The predictions of particle-phase properties involved computations of particle motion in the random velocity field of the continuous phase and are analogous to random-walk calculations. A sufficient number of particle trajectories, allowing for the variation of particle size within a particular nominal particle-size, were computed to obtain statistically significant results.

Computation of particle motion generally followed an approach used earlier for particle-laden jets (Parthasarathy & Faeth 1987). Since particle volume fractions were small, the flow was assumed to be dilute and effects of nearby particles on interphase momentum transport, as well as particle collisions, were neglected. The particles were assumed to be small in comparison to the smallest scales of the turbulence. This is marginal since Kolmogorov lengthscales are in the range 240–390 μm which is somewhat smaller than the particle diameters. Nevertheless, this approximation is reasonable since the turbulent dispersion of particles is dominated by the large-scale energy-containing features of the flow while the terminal velocities of particles in the turbulent environment were not very different from a still liquid. The particles were assumed to be spherical with p.d.f.s of particles diameter taken from figure 1: this is justified by the reasonable estimates of particle terminal velocity distributions using this approach, illustrated in figure 2. Effects of Magnus forces were neglected based on observations during calibration of self-induced motion discussed earlier. Since the flows were homogeneous, Saffman lift forces were neglected while effects of static pressure gradients can be neglected with little error since bath velocities are small in comparison to particle velocities.

Under these assumptions, particle motion can be found using the formulation of Odar & Hamilton (1964), reviewed by Clift *et al.* (1978), as follows:

$$\mathrm{d}x_{\mathrm{p}i}/\mathrm{d}t = u_{\mathrm{p}i}, \tag{6}$$

$$(\rho_{\mathrm{p}}/\rho + \Delta_{\mathrm{A}}/2)\,\mathrm{d}u_{\mathrm{r}i}/\mathrm{d}t = g(\rho_{\mathrm{p}}/\rho - 1)\,\delta_{1i} - 3C_{\mathrm{D}}|u_{\mathrm{r}}|\,u_{\mathrm{r}i}/(4d_{\mathrm{p}}) - \Delta_{\mathrm{H}}(81\nu/\pi d_{\mathrm{p}}^2)^{\frac{1}{2}}\int_{t_0}^{t}(t-\xi)^{-\frac{1}{2}}(\mathrm{d}u_{\mathrm{r}i}/\mathrm{d}\xi)\,\mathrm{d}\xi, \tag{7}$$

where $x_{\mathrm{p}i}$ and $u_{\mathrm{r}i}$ are the particle position and relative velocity (in a Cartesian reference frame with $i = 1$ denoting the vertical direction), t is time, t_0 is the time of the start of motion, δ_{1i} is the Kronecker delta function and Δ_{A} and Δ_{H} are parameters which account for effects of particle acceleration. The terms on the left-hand side of (7) represent the acceleration of the particle and its virtual mass; the terms on the right-hand side represent buoyancy, drag and Basset history forces.

The parameters Δ_{A} and Δ_{H} were empirically correlated by Odar & Hamilton (1964), as follows:

$$\Delta_{\mathrm{A}} = 2.1 - 0.123M_{\mathrm{A}}^2/(1 + 0.12M_{\mathrm{A}}^2), \tag{8}$$

$$\Delta_{\mathrm{H}} = 0.48 + 0.52M_{\mathrm{A}}^3/(1 + M_{\mathrm{A}})^3, \tag{9}$$

where M_{A} is the particle acceleration modulus

$$M_{\mathrm{A}} = (\mathrm{d}u_{\mathrm{r}}/\mathrm{d}t)\,d_{\mathrm{p}}/u_{\mathrm{r}}^2. \tag{10}$$

The values of Δ_{A} and Δ_{H} vary in the ranges 1.0–2.1 and 1.00–0.48, the former values being the correct limit of (7) at the Basset–Boussinesq–Oseen (B–B–O) limit of the formulation (Clift *et al.* 1978). The drag coefficient was found from (2) as noted

earlier: this is reasonable based on the terminal velocity predictions of figure 2 and the fact that liquid velocity fluctuations are small in comparison to particle terminal velocities, i.e. relative turbulent intensities are small. Naturally, use of the Odar & Hamilton (1964) correction factors in a turbulent environment is speculative; however, evaluation of the sensitivity of the predictions to these parameters, to be taken up later, shows that their effect is small for present test conditions in any event.

3.2. *Statistical simulation*

Statistical simulation of particle trajectories was based on statistical time-series simulation techniques adapted from Box & Jenkins (1976). The statistical simulation of the velocity field of the continuous phase can be designed to satisfy any number of the properties of the continuous phase: mean velocities, velocity fluctuations, Lagrangian time correlations, instantaneous conservation of mass, higher-order correlations, etc. However, priorities must be set since computational requirements increase as the number of properties in the flow to be simulated increase. Based on the results of earlier simulations to predict the turbulent dispersion of particles (Faeth 1987), mean and fluctuating velocities and Lagrangian time correlations of velocity fluctuations appear to be sufficient to treat turbulent particle dispersion; therefore, present simulations were designed to reproduce these properties.

The properties of the liquid velocity field were taken from Parthasarathy & Faeth (1990) at the appropriate test conditions. The present flows are homogeneous so that cross-correlations like $\overline{u'v'}$ are small while mean liquid velocities are also small and do not affect particle velocity fluctuations; therefore, only liquid velocity fluctuations must be simulated and velocity components can be assumed to be statistically independent. However, liquid velocity fluctuations are not isotropic (see table 2) with streamwise velocity fluctuations being roughly twice cross-stream velocity fluctuations (both components of which are equal). Finally, measurements showed that liquid velocity fluctuations satisfied Gaussian p.d.f.s (Parthasarathy & Faeth 1990).

To illustrate the approach used to simulate liquid velocities along a particle path, consider a simulation using equal timesteps, Δt, that has proceeded $i-1 > p > 0$ timesteps. The value of any component of the liquid velocity fluctuations at the location of the particle at the end of the next timestep, say u_i' (where u can be any velocity component and i denotes the timestep) is found from the following autoregressive process (Box & Jenkins 1976):

$$u_i' = \sum_{j=p}^{i-1} A_{ij} u_j' + a_i \quad (1 \leqslant p \leqslant i-1). \tag{11}$$

In (11) the A_{ij} are weighting factors so that correlations at various times can be satisfied, a_i is an uncorrelated random variable having a Gaussian p.d.f. chosen so that the p.d.f. of u_i' is satisfied, and p is selected to eliminate points having small correlation coefficients with respect to the point i. The A_{ij} are related to correlations of liquid velocity fluctuations through the Yule–Walker equations, as follows (Box & Jenkins 1976):

$$\overline{u_i' u_k'} = \sum_{j=p}^{i-1} A_{ij} \overline{u_j' u_k'} \quad (k = p, \ldots, i-1). \tag{12}$$

The first moment of a_i is zero while the second moment is found from the following expression

$$\overline{a_i^2} = \overline{u_i'^2} - \sum_{j=p}^{i-1} A_{ij} \overline{u_i' u_j'}. \tag{13}$$

Given the correlations $\overline{u_i' u_k'}$, etc. (12) is a positive-definite linear system of equations which can be readily solved using Cholesky factorization. The a_i^2 can then be found from (13) since all quantities on the right-hand side of this equation are known.

For present flows, it will be shown that the correlations are roughly exponential; then, Box & Jenkins (1976) show that (12) can be reduced to a Markov process where only a single previous timestep must be considered to find u_i', as follows:

$$u_i' = A_{ii-1} u_{i-1}' + a_i, \tag{14}$$

where A_{ii-1} is the correlation $\overline{u_i' u_{i-1}'}$. Then a_i is found from a Gaussian distribution with a zero mean value and a variance from (13) as follows:

$$\overline{a_i^2} = (1 - A_{ii-1}^2)\,\overline{u_i'^2}. \tag{15}$$

At this limit, the simulation becomes a Uhlenbeck–Ornstein (OU) process, which has been used in past studies of turbulent dispersion of fluid particles (Durbin 1980; Anand & Pope 1985; Sawford & Hunt 1986).

The simulation begins with a random selection of the components of the velocity fluctuations at the initial condition, u_0'; satisfying Gaussian p.d.f.s having the measured variances and degree of anisotropy. $\overline{a_1^2}$ can then be found from (15). A random selection of a_1 from its p.d.f. then yields u_1' from (14). After repeating this process to find all three velocity components, the motion of the particle in this velocity field is computed by integrating (6) and (7) to find particle properties at Δt. The calculation continues in this manner for additional increments of time until particle properties becomes statistically stationary. For present computations, 5000 trajectories of this type were considered to find final results, with the sizes of the 5000 particles distributed according to the particle size distributions illustrated in figure 1.

Liquid velocity fluctuations were known directly from the measurements of Parthasarathy & Faeth (1990). Thus, the key to simulating particle trajectories is knowledge of the Lagrangian correlations, A_{ii-1}. Fortunately, although Taylor's hypothesis is not appropriate to relate temporal and spatial variations of turbulence properties at a fixed point, since mean liquid velocities were small, it could be applied to obtain correlations along a particular path, since the relative velocities of the particles were large in comparison to velocity fluctuations. Thus, knowledge of spatial and temporal correlations in the streamwise direction from Parthasarathy & Faeth (1990) allowed the A_{ii-1} to be estimated and showed that departures from Taylor's hypothesis were small. In particular, the Lagrangian correlation of streamwise liquid velocity fluctuations along a particle path was obtained from the measured streamwise correlation of liquid velocity fluctuations, as follows:

$$\overline{u_{xi}' u_{xi-1}'} \approx \overline{u_x'(x + U_\infty\, i\,\Delta t, t)\, u_x'(x + U_\infty (i-1)\,\Delta t, t)} = \overline{u_x'(x,t)\, u_x'(x + U_\infty \Delta t, t)}, \tag{16}$$

where x and u_x are the streamwise direction and liquid velocity. The correlation coefficients needed to find the correlations of (16) are plotted as a function of $\Delta t/\tau_L$, where τ_L is the Lagrangian integral timescale, in figure 3. The measurements of Parthasarathy & Faeth (1990) at the low and high loadings of the three particle sizes, as well as the exponential approximation, $\exp(-\Delta t/\tau_L)$, are shown on the figure. The exponential approximation is seen to provide a reasonably good fit of the measurements within experimental uncertainties (estimated to be less than 36%). Naturally, this comes about largely due to the inability of the measurements to resolve the shortest lengthscales of the flow owing to problems of step-noise, where the correlation departs from exponential behaviour (Parthasarathy & Faeth 1990).

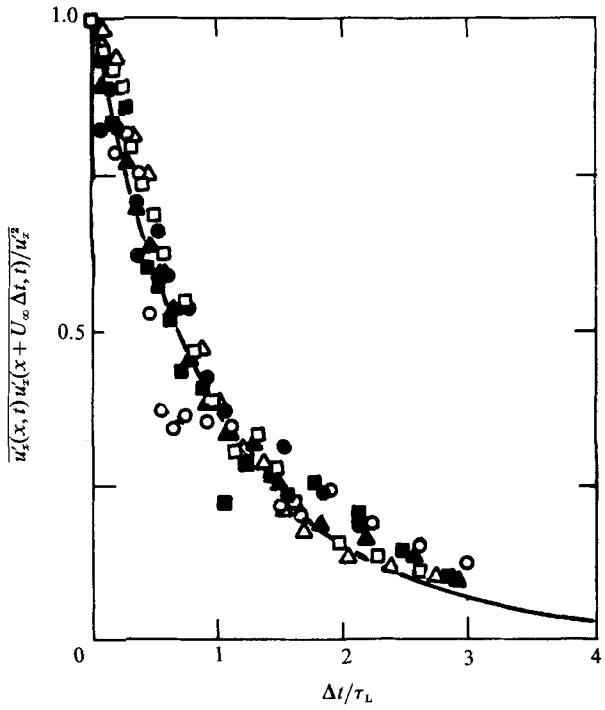

FIGURE 3. Lagrangian temporal correlations of streamwise liquid velocity fluctuations along a particle path. $d_p = 0.5$ mm: □, ■, low and high loadings; $d_p = 1.0$ mm: ○, ●, low and high loadings; $d_p = 2.0$ mm: △, ▲, low and high loadings; ——, $\exp(-\Delta t/\tau_L)$ approximation.

However, particle motion is primarily influenced by liquid motions having large scales so that this deficiency is not a major problem for present purposes. Based on the results of Parthasarathy & Faeth (1990) the values of τ_L are 0.91, 0.40 and 0.22 s for the 0.5, 1.0 and 2.0 mm diameter particles.

The simulation requires knowledge of the Lagrangian correlations of cross-stream liquid velocities as well. Unfortunately, spatial correlations of cross-stream liquid velocities in the streamwise direction were not measured by Parthasarathy & Faeth; therefore, they were assumed to vary in the same manner as the spatial correlations of liquid streamwise velocities for lack of an alternative The output of the stochastic simulation consisted of particle properties like $\tilde{u}_p$, $\tilde{v}_p$, $\tilde{u}_p''^2$ and $\tilde{v}_p''^2$ – the latter two being direct measures of the effects of turbulent particle dispersion.

4. Results and discussion

4.1. *Velocities*

Measured and predicted particle properties included mean and fluctuating velocities and velocity probability density functions. These results are considered in the following, concluding with a study of the sensitivity of the predictions to parameters of the formulation.

Measurements of mean streamwise and fluctuating streamwise and cross-stream particle velocities are illustrated in figure 4. The velocities are plotted as a function of the rate of dissipation, which is the main variable controlling liquid velocity fluctuations (Parthasarathy & Faeth 1990), for the 0.5, 1.0 and 2.0 mm diameter

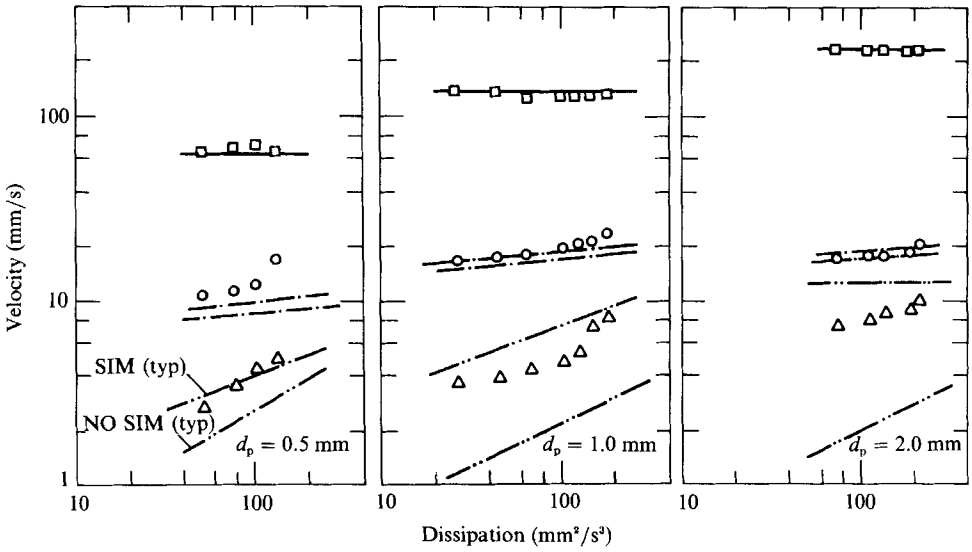

FIGURE 4. $\tilde{u}_p$: □, data; ——, prediction; $(\tilde{u}_p''^2)^{\frac{1}{2}}$: ○, data; —·—, prediction; $(\tilde{v}_p''^2)^{\frac{1}{2}}$: △, data; —··—, prediction.

particles. A range of particle loadings (or values of ϵ) are considered, rather than just the loadings for each particle size summarized in table 2, so that the trends of the measurements can be observed more readily.

Measurements of mean particle velocities illustrated in figure 4 do not exhibit any systematic variation with dissipation and are identical to the terminal velocities of the particles within experimental uncertainties (see table 2). In contrast, evidence for changes of mean particle velocities in particle-generated flows or homogeneous turbulent fields is provided by the theoretical studies of Batchelor (1972) and Maxey (1987). Batchelor (1972) considers the sedimentation of particles having Reynolds numbers in the Stokes regime, finding that settling velocities decrease as the particle volume fractions increase. Aside from the fact that present particle Reynolds numbers are greater than 38, which is well beyond the Stokes regime so that the applicability of these results is questionable, present particle volume fractions are also low, less than 0.01%, so that changes estimated from Batchelor's findings are less than 0.1% and are not significant in comparison to experimental uncertainties. Maxey (1987) considers dilute particle flows in a homogeneous turbulent field, also at Stokes limit. He finds that settling velocities should increase in the presence of turbulence, however, the effect becomes relatively small when the ratio of the mean particle velocity to the continuous-phase velocity fluctuations exceeds 2. For present test conditions, this ratio is in the range 13–71 so that changes in settling velocities due to this mechanism should be small as well.

Thus, due to small particle volume fractions, and large settling velocities in comparison to levels of turbulent fluctuations, it is not surprising that there was little difference between settling velocities in turbulent and non-turbulent environments for the present test conditions. However, additional evaluation of factors influencing settling velocities beyond the Stokes regime would be desirable. Furthermore, the picture could change at higher particle loadings than those considered here. For example, liquid velocity fluctuations are proportional to $\epsilon^{\frac{1}{3}}$ (Parthasarathy & Faeth 1989) so that large particle loadings could yield velocity fluctuations comparable to

Particle diameter (mm)	0.5		1.0		2.0	
Particle loading	Low	High	Low	High	Low	High
$(\tilde{u}''^2_{ps}/\overline{u}'^2)^{\frac{1}{2}}$	0.6	0.4	0.6	0.3	0.1	0.1
$(\tilde{u}''^2_{pt}/\overline{u}'^2)^{\frac{1}{2}}$	2.0	1.4	5.9	2.8	4.3	2.6
$(\tilde{u}''^2_{p}/\overline{u}'^2)^{\frac{1}{2}}$	3.3	2.6	7.1	4.3	5.1	3.4
$(\tilde{v}''^2_{ps}/\overline{v}'^2)^{\frac{1}{2}}$	0.7	0.4	4.7	2.4	7.9	4.4
$(\tilde{v}''^2_{p}/\overline{v}'^2)^{\frac{1}{2}}$	1.7	1.6	2.1	3.2	4.6	3.2

TABLE 3. Ratios of particle/liquid velocity fluctuations

settling velocities. Particle concentrations at such conditions would be very high, however, more like fluidized bed processes, so that such flows would not be dilute and extrapolation of present results to these conditions would be very questionable. Nevertheless, the evolution between the present dilute particle flows and fluidized bed conditions has interesting implications for a better understanding of both flows and merits further study.

The particle velocity fluctuations illustrated in figure 4 are influenced by several phenomena, as follows: self-induced particle motion, apparent streamwise velocity fluctuations due to the variation of terminal velocities over the size range of the present experiments, and turbulent dispersion of the particles. Results summarized in table 3 help provide some insight into the relative importance of these phenomena for present test conditions. This table is a summary of the ratios of particle velocity fluctuations normalized by the corresponding component of bath liquid velocity fluctuations. Test conditions include low and high loadings for all three particle sizes. Streamwise and cross-stream velocity fluctuations are considered for self-induced motion $(\tilde{u}''^2_{ps})^{\frac{1}{2}}$ and $(\tilde{v}''^2_{ps})^{\frac{1}{2}}$ (obtained by calibration) and motion within the bath itself, $(\tilde{u}''^2_{p})^{\frac{1}{2}}$ and $(\tilde{v}''^2_{p})^{\frac{1}{2}}$. However, only the streamwise apparent velocity fluctuations due to particle size variations $(\tilde{u}''^2_{pt})^{\frac{1}{2}}$ (obtained by calibration) have been considered since this is the only velocity component that is relevant for this effect.

Comparing the velocity fluctuation ratios listed in table 3 for self-induced motion and terminal velocity variations with those measured in the bath provides a relative measure of the importance of these effects in comparison with turbulent dispersion. It is seen that streamwise velocity fluctuations due to self-induced motion are small while apparent fluctuations due to terminal velocity variations are comparable to those measured in the bath; therefore, streamwise particle velocity fluctuations are dominated by effects of terminal velocity variations due to variations of particle diameter for present test conditions and relatively little can be learned about turbulent dispersion from this velocity component. A possible exception is the highest loading with the 0.5 mm diameter particles where effects of terminal velocity variations are roughly half the velocity fluctuation levels observed in the bath; nevertheless, reduced sensitivity due to direct effects of turbulent dispersion still makes this condition marginal for definitive conclusions. The results for cross-stream velocity fluctuations suggest that effects of self-induced motion are relatively small in comparison to turbulent dispersion for the 0.5 mm diameter particles; therefore, this condition provides a reasonable indication of effects of turbulent dispersion. In contrast, cross-stream velocity fluctuations due to self-induced particle motion are generally larger than those observed in the bath for the 1.0 and 2.0 mm diameter particles so that these test conditions are of questionable value for gaining information about turbulent dispersion. A curious phenomena is that cross-stream

velocity fluctuations observed in the bath for the larger sizes are smaller than those observed during the calibration tests for self-induced particle motion in still liquids. This suggests that the turbulent field of the bath is interfering with eddy-shedding that is thought to cause this behaviour. Additional study of this effect under more controlled conditions would be desirable.

The previous considerations imply that turbulent dispersion is the dominant process causing particle velocity fluctuations only for the cross-stream velocity fluctuations with the 0.5 mm diameter particles for present test conditions. In this case, the ratio of particle to liquid cross-stream velocity fluctuations are in the range 1.6–1.7 (see table 3) which implies that particle velocities overshoot liquid velocities. Similarly, if the contribution of terminal velocity variations is subtracted from the streamwise velocity fluctuations measured in the bath the result still yields particle streamwise velocity fluctuations greater than the liquid streamwise velocity fluctuations for the 0.5 mm diameter particles. This occurs since particle response varies over the spectra of the continuous-phase velocity fluctuations and depending upon the energy content of the range of frequencies where the response is greatest the particle fluctuations can be greater or smaller than a single measure of liquid-phase velocity fluctuations such as the root-mean squared velocity fluctuation. The results also suggest that turbulent dispersion is very effective in the homogeneous turbulence field generated by the particles themselves. This behaviour is caused by the large frequency range of the continuous-phase velocity fluctuations since both mean and turbulent wake properties contribute to the spectra, see Parthasarathy & Faeth (1990). With such a large range of frequencies available, the probability that the particles will encounter a range of frequencies where their response is high is enhanced – enhancing effects of turbulent dispersion as well. In particular, particle response tends to be highest (approaching unity) at low frequencies (Al Taweel & Landau 1977). Thus, the high signal energy content at low frequencies due to effects of mean wake velocities is probably a significant factor in the good turbulent dispersion properties of present homogeneous particle-laden flows.

Combining an efficient mechanism of turbulent dispersion with effects of self-induced motion and variations of terminal velocities, generally yields particle velocity fluctuations that are greater than liquid velocity fluctuations (as much as 5.5 times greater) over the present test range. Thus, when considering effects of turbulent dispersion, intuitive ideas that particles will have some difficulty in responding to liquid-phase fluctuations owing to their inertia, and will necessarily mix more slowly than an infinitely-small particle as a result, should be accepted with caution.

Effects of loading (dissipation) on particle velocity fluctuations can be seen best in figure 4. Streamwise particle velocity fluctuations are large, and do not vary very much with dissipation, since they are dominated by variations of terminal velocities over the present test range (the highest loading for the 0.5 mm diameter particles exhibits a greater effect but measurements are also least accurate at this condition since particle concentrations are greatest). In contrast, cross-stream particle velocity fluctuations are significantly increased with increasing rates of dissipation for all particle sizes. As just discussed, this increase can be attributed to effects of turbulent dispersion for the 0.5 mm diameter particles. In fact, noting that the ratio of $(\tilde{v}_{\mathrm{p}}''^2)^{\frac{1}{2}}/(\overline{v'^2})^{\frac{1}{2}}$ is roughly constant, indicating similar particle response to cross-stream liquid velocity fluctuations over the present test range (see table 3), this increase simply follows the $\epsilon^{\frac{1}{2}}$ variation of liquid velocity fluctuations. Surprisingly, the cross-stream particle velocity fluctuations also exhibit significant increases with increasing

dissipation for the 1.0 and 2.0 mm diameter particles even though these results should be dominated by self-induced lateral motion of the particles (see table 3). This suggests that eddy-shedding mechanisms leading to self-induced lateral motion in still liquids may be less effective in turbulent environments so that effects of turbulent dispersion are greater than might be anticipated from the results summarized in table 3.

Predictions based on the present stochastic analysis of the particle phase are also illustrated in figure 4. Recall that these predictions are based on the measured turbulence properties of the liquid phase and that effects of particle size variations are considered; however, effects of self-induced motion of the particles have been ignored since no information is available concerning the fluctuating forces on the particles due to irregular particle shapes and eddy-shedding. In an effort to provide some indication of potential effects of self-induced particle motion, predictions are shown where mean-squared particle velocity fluctuations from the particle trajectory simulations and the self-induced motion are vectorially added, i.e. $\tilde{u}_{\mathrm{p}}''^2 = \tilde{u}_{\mathrm{p\,pred}}''^2 + \tilde{u}_{\mathrm{ps}}''^2$, etc.: these predictions are denoted SIM to indicate that 'self-induced motion' has been considered. The baseline predictions without consideration of self-induced motion are denoted by NO SIM.

Mean velocity predictions are in excellent agreement with measurements in figure 4. This is not a very critical test of predictions, however, since the predictions largely reflect the correct calibration of particle drag properties which was discussed earlier. The new features that the simulations include is the increase of mean particle drag properties by turbulent fluctuations, i.e. computing particle drag using average liquid-phase properties is not correct since drag is not a linear function of the relative velocity for Reynolds number greater than unity (Faeth 1987); and the biasing of particle motion by interactions with the turbulent field analogous to the properties investigated by Maxey (1987). These factors are considered by the simulations because drag is based on instantaneous relative velocities and the turbulent field is simulated through second-order correlations. Nevertheless, neither effect influences mean particle velocities significantly for present test conditions since mean particle velocities are much greater than liquid velocity fluctuations: the relative turbulence intensities never exceeded 8% so that biasing of drag is small while the turbulent interaction effect is not likely to be significant based on the results of Maxey (1987) discussed earlier.

Predicted streamwise particle velocity fluctuations in figure 4 generally agree with measurements within experimental uncertainties. In this case, the fluctuations are dominated by the effects of variations of terminal velocities and effects of self-induced motion are small (see table 3). Nevertheless, it is encouraging that the relatively small increase of particle velocity fluctuations due to increased turbulent dispersion with increasing dissipation is represented quite well by the predictions.

The comparison between predicted and measured cross-stream velocity fluctuations in figure 4 is hampered by effects of self-induced particle motion. However, this effect is modest for the 0.5 mm diameter particles and the baseline predictions (NO SIM) are reasonably good while the present *ad hoc* correction for self-induced particle motion yields results (SIM) that are in excellent agreement with measurements. This suggests that the most important properties of the turbulent field have been considered and that effects of turbulence on particle drag are modest. The last observation is reasonable since the relative velocities of the particles are large in comparison to liquid phase velocity fluctuations, i.e. relative turbulence intensities are small as noted earlier. Predictions ignoring self-induced motion show

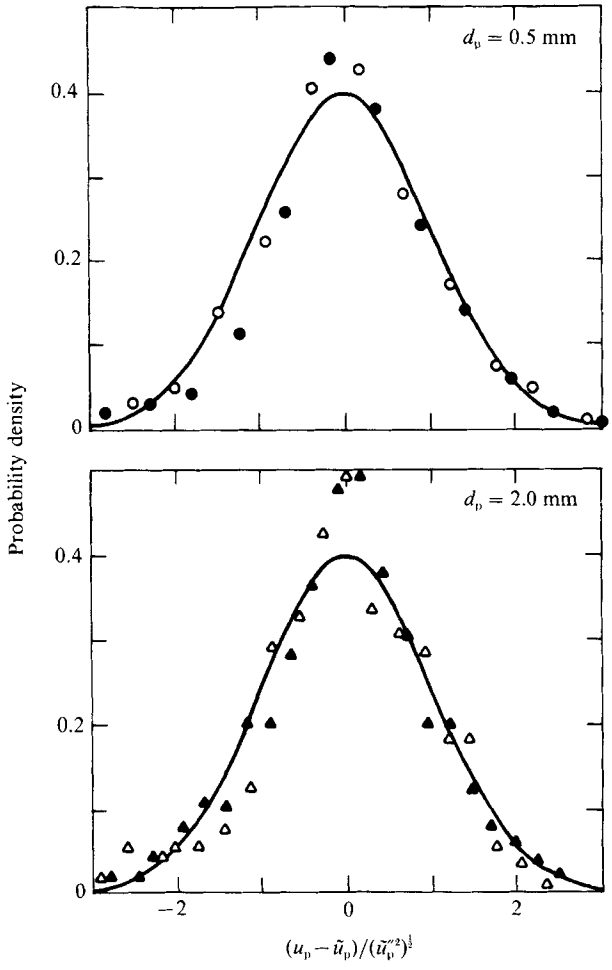

FIGURE 5. Probability density functions of streamwise particle velocity fluctuations. d_p = 0.5 mm: ○, ●, low and high loadings; d_p = 2.0 mm: △, ▲, low and high loadings; ——, prediction.

a progressive reduction of cross-stream particle velocity fluctuations with increasing particle diameter at the same value of ϵ. This behaviour follows since liquid velocity fluctuations only depend on ϵ for present test conditions (Parthasarathy & Faeth 1990) while increased particle diameter reduces the response of the particles to liquid velocity fluctuations. Effects of self-induced motion tend to overwhelm this trend, however, so that predictions ignoring self-induced motion are much smaller than the measurements for the 1.0 and 2.0 mm diameter particles while including the self-induced motion causes cross-stream particle velocity fluctuations to be over-estimated. This highlights the need to develop a rational method of including the self-induced forces on the particles in particle trajectory calculations. As noted earlier, the results suggest that the turbulent flow field may be modifying eddy-shedding mechanisms responsible for self-induced particle motion as well.

4.2. *Probability density functions*

The probability density functions of streamwise particle velocity fluctuations are plotted as a function of normalized variables in figure 5. Measurements for the different loadings of the 0.5 and 2.0 mm diameter particles appear on the plots. These

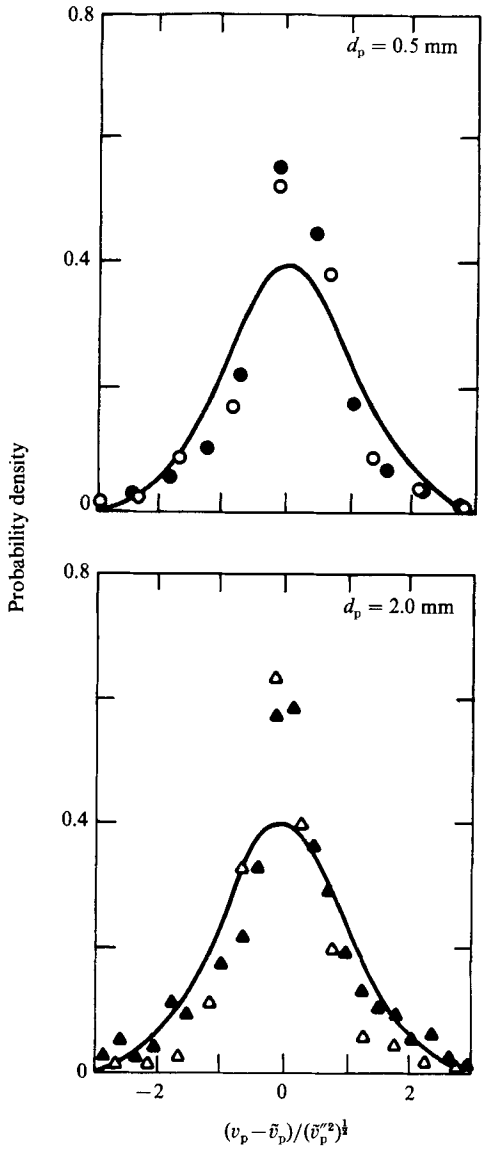

FIGURE 6. Probability density functions of cross-stream particle velocity fluctuations. Identification of symbols the same as figure 5.

measurements are not significantly different from the particle drag calibrations, since particle velocity fluctuations in the streamwise direction are dominated by terminal velocity variations. Thus, predictions both considering and ignoring self-induced motion are very nearly the same and are in reasonably good agreement with the measurements, particularly since the results are normalized. The predictions essentially yield Gaussian probability density functions.

The probability density functions of cross-stream particle velocity fluctuations are illustrated in figure 6. The method of plotting and test conditions are the same as figure 5. Owing to the method of normalization, results for the 0.5 mm diameter particles (which are dominated by effects of turbulent dispersion) are essentially the

Input parameter (100% change)	Change of output parameter (%)		
	$\tilde{u}_p$	$(\tilde{u}_p''^2)^{\frac{1}{2}}$	$(\tilde{v}_p''^2)^{\frac{1}{2}}$
$(\tilde{u}'^2)^{\frac{1}{2}}$	~ 0	20 to 24	~ 0
$(\tilde{v}'^2)^{\frac{1}{2}}$	~ 0	~ 0	98 to 100
τ_L	~ 0	0 to 4	~ 0
C_D	-32 to -39	-28 to -32	~ 0

TABLE 4. Results of sensitivity study of particle properties. These results were similar for the 0.5, 1.0 and 2.0 mm diameter particles over the present range of particle loadings; therefore, only the range of output changes are shown. Use of standard values or $\Delta_A = \Delta_H = 0$ resulted in negligible changes of predictions.

same as results for larger particles (which are dominated by effects of self-induced particle motion). Similarly, the various predictions are nearly the same and all of the predictions approximate Gaussian probability density functions. The flatness factors of the measured probability density functions of the cross-stream velocity fluctuations are: 4.7 and 5.3 for the low and high loadings of the 0.5 mm particles; and 6.3 and 3.5 for the low and high loadings of the 2 mm particles. Thus, these measurements depart from a Gaussian distribution which would have a flatness factor of 3. A possible reason for this behaviour is that self-induced motion may inhibit Gaussian behaviour, but more study is needed to understand the effects of self-induced particle motion on particle motion before any firm conclusions can be drawn.

4.3. *Sensitivity study*

The numerical simulations of particle motion required the prescription of a number of parameters subject to significant uncertainties, as follows: the liquid velocity fluctuations, the Lagrangian integral timescale, the particle drag coefficient, and the virtual mass and Basset history force parameters of (8) and (9). In order to better understand the nature and limitations of the numerical simulation, the sensitivity of predictions to variations of these parameters was studied.

Results of the sensitivity study appear in table 4 where changes in output parameters for 100% changes in input parameters are summarized. Effects of particle size variations were considered during these computations but not effects of self-induced particle motion. These results were similar for all three particle sizes over the range of loadings considered during this investigation; therefore, only the range of output variable changes are shown. Predicted mean streamwise particle velocities were only sensitive to estimates of particle drag coefficients, where 100% changes of C_D yielded 30–40% changes of the particle mean velocity. This behaviour is expected since terminal velocities of the particles were not influenced strongly by the bath turbulence and are proportional to $C_D^{-\frac{1}{2}}$, see (1).

Predicted streamwise particle velocity fluctuations were primarily influenced by changes of the drag coefficient and streamwise liquid velocity fluctuations. The effect of drag coefficient is the same as for mean particle velocities – for the same reasons. The effect of a 100% increase of liquid velocity fluctuations on streamwise particle velocity fluctuations was only 20–24%: this follows since streamwise particle velocity fluctuations were dominated by variations of particle terminal velocities due to size variations for present test conditions. The small effect of cross-stream liquid velocity fluctuations on streamwise particle velocity fluctuations occurs since this variable primarily influences streamwise properties by modifying particle drag

coefficients; therefore, its effect is not large since particle terminal velocities are much greater than liquid velocity fluctuations for present test conditions. The insensitivity to variations of the Lagrangian integral timescale, τ_L, follows since this variable is most closely associated with effects of turbulent dispersion that are small for this component of velocity.

Predicted cross-stream particle velocity fluctuations were really only influenced by variations of cross-stream liquid velocity fluctuations, where the changes of the output have a one-to-one correspondence with changes of the input. This highlights the strong interaction between the particles and the turbulence of the liquid phase for present test conditions, causing very effective turbulent dispersion, i.e. cross-stream particle velocity fluctuations are greater than liquid velocity fluctuations in the cross-stream direction. The insensitivity to streamwise liquid velocity fluctuations follows for the same reasons that cross-stream liquid velocity fluctuations had little effect on streamwise particle velocity fluctuations. The insensitivity to both τ_L and C_D are probably related. The effective turbulent dispersion for present conditions implies that particles have sufficiently high drag to respond quite closely to the lateral liquid velocity fluctuations; therefore, additional time to respond is not needed while increasing the drag coefficient only serves to reduce already small relative velocities in the cross-stream direction.

Finally, effects of using either of the standard values Δ_A and Δ_H or setting these parameters equal to zero was small. This follows since mean particle velocities are not influenced by particle size variations, and particle response in the cross-stream direction is very high and is relatively insensitive to parameters that influence particle drag properties.

5. Conclusions

The present investigation considered the turbulent dispersion of particles in their self-generated homogeneous turbulent field. The specific configuration involved nearly monodisperse glass spheres (particle diameters of 0.5, 1.0 and 2.0 mm with corresponding Reynolds number of 38, 156 and 545) falling with constant particle number fluxes in a water bath under dilute conditions (particle volume fractions less than 0.01%). The major observations and conclusions of the study are as follows:

(i) Present particles exhibited drag coefficients that were within 14% of the standard drag curve for spheres, in spite of some ellipticity of their shapes. However, individual particles falling in motionless water exhibited self-induced motion, particularly in the lateral direction. Self-induced motion increased with increasing particle size due to both eddy-shedding at large particle Reynolds numbers as well as increased ellipticity of the larger particles.

(ii) Mean particle velocities were independent of dissipation and approached the terminal velocity of the particles in a still liquid since liquid volume fractions were small and particle settling velocities were large in comparison to liquid velocity fluctuations.

(iii) Particle velocity fluctuations exceeded liquid velocity fluctuations for all test conditions. Large streamwise particle velocity fluctuations were dominated by modest particle size differences resulting in variations of terminal velocities. Cross-stream velocity fluctuations were due to turbulent dispersion, which is effective in this flow since integral scales are relatively large, enhanced by effects of self-induced motion for the larger particles. However, effects of self-induced motion were smaller in the particle-generated turbulent field than in still liquids, suggesting that

turbulence may interfere with eddy-shedding mechanisms thought to be responsible for this behaviour.

(iv) Stochastic simulation of particle motion, allowing for probability density functions of liquid velocity fluctuations and Lagrangian temporal correlations, yielded encouraging results. This indicates that use of statistical time-series techniques to simulate liquid-phase properties provides a useful simplification to treat turbulent dispersion since it eliminates many of the *ad hoc* features of earlier simplified methods while avoiding the extensive computations needed for full numerical simulation of the flow.

The authors wish to thank L. P. Bernal and W. W. Willmarth for helpful discussions during the course of the study. The work was supported by the Air Force Office of Scientific Research, Grant no. AFOSR-85-0244, under the technical management of J. M. Tishkoff. The US Government is authorized to reproduce and distribute copies of this paper for Governmental purposes notwithstanding any copyright notation thereon.

REFERENCES

Al Taweel, A. M. & Landau, J. 1977 Turbulence modulation in two-phase jets. *Intl J. Multiphase Flow* **3**, 341–351.

Anand, M. A. & Pope, S. B. 1985 Diffusion behind a line source in grid turbulence. *Fourth Symposium on Turbulent Shear Flows*, pp. 17.11–17.17.

Batchelor, G. K. 1972 Sedimentation in a dilute dispersion of spheres. *J. Fluid Mech.* **52**, 245–268.

Box, G. E. P. & Jenkins, G. M. 1976 *Time Series Analysis*, rev. edn, pp. 47–84. Holden Day.

Clift, R., Grace, J. R. & Weber, M. E. 1978 *Bubbles, Drops and Particles*, pp. 266–269, 296–302. Academic.

Crowe, C. T. 1982 Review – numerical models for dilute gas particle flows. *J. Fluids Engng* **104**, 297–303.

Csanady, G. T. 1963 Turbulent diffusion of heavy particles in the atmosphere. *J. Atmos. Sci.* **20**, 201–208.

Desjonqueres, P., Gouesbet, G., Berlemont, A. & Picart, A. 1986 Dispersion of discrete particles by continuous turbulent motions: new results and discussions. *Phys. Fluids* **29**, 2147–2151.

Durbin, P. A. 1980 A random flight model of inhomogeneous turbulent dispersion. *Phys. Fluids* **23**, 2151–2153.

Faeth, G. M. 1987 Mixing, transport and combustion in sprays. *Prog. Energy Combust. Sci.* **13**, 293–345.

Ferguson, J. R. & Stock, D. E. 1986 Particle dispersion in decaying isotropic homogeneous turbulence. *Gas–Solid Flows* (ed. J. J. Jurewicz), pp. 9–14. ASME.

Gouesbet, G., Berlemont, A. & Picart, A. 1984 Dispersion of discrete particles by continuous turbulent motions. Extensive discussion of the Tchen's theory using a two-parameter family of Lagrangian correlation functions. *Phys. Fluids* **27**, 827–837.

Katz, E. J. 1966 Atmospheric diffusion of settling particles with sluggish response. *J. Atmos. Sci.* **23**, 159–166.

Kraichnan, R. H. 1970 Diffusion by a random velocity field. *Phys. Fluids* **13**, 22–31.

Maxey, M. R. 1987 The gravitational settling of aerosol particles in homogeneous turbulence and random flow fields. *J. Fluid Mech.* **174**, 441–465.

Meek, C. C. & Jones, B. G. 1973 Studies of the behavior of heavy particles in a turbulent fluid flow. *J. Atmos. Sci.* **30**, 239–244.

Nakamura, I. 1976 Steady wake behind a sphere. *Phys. Fluids* **19**, 5–8.

NIR, A. & PISMEN, L. M. 1979 The effect of a steady drift on the dispersion of a particle in a turbulent fluid. *J. Fluid Mech.* **94**, 369–381.

ODAR, F. & HAMILTON, W. S. 1964 Force on a sphere accelerating in a viscous fluid. *J. Fluid Mech.* **18**, 302–314.

PARTHASARATHY, R. N. 1989 Homogeneous dilute turbulent particle-laden water flows. PhD thesis, The University of Michigan.

PARTHASARATHY, R. N. & FAETH, G. M. 1987 Structure of particle-laden turbulent water jets in still water. *Intl J. Multiphase Flow* **13**, 699–716.

PARTHASARATHY, R. N. & FAETH, G. M. 1900 Turbulence modulation in homogeneous dilute particle-laden flows. *J. Fluid Mech.* **220**, 485–514.

PICART, A., BERLEMONT, A. & GOUESBET, G. 1986 Modelling and predicting turbulence fields and dispersion of discrete particles transported by turbulent flows. *Intl J. Multiphase Flow* **12**, 237–261.

PISMEN, L. M. & NIR, A. 1978 On the motion of suspended particles in stationary homogeneous turbulence. *J. Fluid Mech.* **84**, 193–206.

PUTNAM, A. 1961 Integrable form of droplet drag coefficient. *Am. Rocket Soc. J.* **31**, 1467–1468.

REEKS, M. W. 1977 On the dispersion of small particles suspended in an isotropic turbulent fluid. *J. Fluid Mech.* **83**, 529–546.

REEKS, M. W. 1980 Eulerian direct interaction applied to the statistical motion of particles in a turbulent fluid. *J. Fluid Mech.* **97**, 569–590.

SAWFORD, B. L. & HUNT, J. C. R. 1986 Effects of turbulence structure, molecular diffusion and source size on scalar fluctuations in homogeneous turbulence. *J. Fluid Mech.* **165,** 373–400.

SNYDER, W. H. & LUMLEY, J. L. 1971 Some measurements of particle velocity auto-correlation functions in a turbulent flow. *J. Fluid Mech.* **48**, 41–71.

VIETS, H. 1971 Accelerating sphere–wake interaction. *AIAA J.* **9**, 2087–2089.

WELLS, M. R. & STOCK, D. E. 1983 The effects of crossing trajectories on the dispersion of particles in turbulent flow. *J. Fluid Mech.* **136**, 31–62.

YUDINE, M. I. 1959 Physical considerations on heavy-particle diffusion. *Adv. Geophys.* **6**, 185–191.